International Journal of Pharmaceutical research and Applications
Volume 11, Issue 5, Sep.-Oct.2026, pp:760-775 www.ijprajournal.com ISSN:2456-4494

Formulation and Evaluation of Rivaroxaban-Loaded Solid Self-Nanoemulsifying Drug Delivery System (S-SNEDDS) for Dissolution Enhancement

Bharathuvaraj S[1*], Dr. J. Bagyalakshmi[2*]
Department of Pharmaceutics, Sri Ramakrishna Institute of Paramedical Sciences, College of Pharmacy, Coimbatore – 641044, Tamil Nadu, India (affiliated to The Tamil Nadu Dr. M.G.R. Medical University, Chennai)

Date of Submission: 01-10-2026 Date of Acceptance: 11-10-2026

ABSTRACT: Rivaroxaban, a Biopharmaceutics Classification System (BCS) Class II direct Factor Xa inhibitor, exhibits poor aqueous solubility that limits its dissolution and oral bioavailability. The present study aimed to develop and evaluate a solid self-nanoemulsifying drug delivery system (S-SNEDDS) of rivaroxaban to enhance its dissolution. Oleic acid, Tween 80 and PEG 400 were selected as the oil, surfactant and co-surfactant, respectively, on the basis of solubility and emulsification efficiency, and a pseudo-ternary phase diagram was constructed to identify the self-nanoemulsifying region at an Smix ratio of 1:2. Nine liquid SNEDDS formulations (F1–F9) were prepared over an oil-to-Smix ratio of 1:9 to 9:1 and characterized for thermodynamic stability, robustness to dilution, self-emulsification time, viscosity, percentage transmittance, droplet size, polydispersity index (PDI), zeta potential and drug loading efficiency. Formulation F3 (oil:Smix, 3:7) was selected as optimized, showing a droplet size of 95.3 nm, PDI of 0.257, zeta potential of −41.4 mV, transmittance of 99 ± 0.52% and drug loading efficiency of 98.43 ± 0.02%. F3 was converted into S-SNEDDS by adsorption onto Aerosil® 200 (1:2, v/w). The S-SNEDDS exhibited satisfactory micromeritic properties (angle of repose 26.59°, Carr's index 17.2%, Hausner's ratio 1.20) and a drug loading efficiency of 95.43 ± 0.02%. In vitro dissolution testing (USP Apparatus II, phosphate buffer pH 6.8) showed 97.24 ± 0.74% drug release at 60 min from the optimized S-SNEDDS, compared with 50.0 ± 2.5% for pure drug and 75.0 ± 2.7% for a marketed tablet. Release-kinetic modelling indicated the best fit with the first-order model (R^2 = 0.9676). These findings suggest that adsorption-based S-SNEDDS is a practical formulation strategy for enhancing the in vitro dissolution of rivaroxaban and may serve as a basis for further bioavailability evaluation.

KEYWORDS: Rivaroxaban; Solid SNEDDS; Self-Nanoemulsifying Drug Delivery System; Adsorption Technique; Dissolution Enhancement; Pseudo-Ternary Phase Diagram; First-Order Kinetics.

I. INTRODUCTION

Oral administration remains the most widely used and patient-preferred route of drug delivery, yet its clinical success depends on a drug's ability to dissolve and permeate the gastrointestinal epithelium in adequate concentration. Nearly 40–70% of new chemical entities emerging from contemporary drug-discovery pipelines display poor aqueous solubility, a large proportion of which fall under Class II or Class IV of the Biopharmaceutics Classification System (BCS) [1,2]. For such drugs, dissolution rather than permeability is the rate-limiting step governing systemic absorption, as described by the classical Noyes–Whitney relationship between saturation solubility, diffusion layer thickness and dissolution rate [3].

Rivaroxaban is an orally active, direct Factor Xa inhibitor used for the prevention and treatment of venous thromboembolism, stroke prevention in non-valvular atrial fibrillation, and related thrombotic indications [4,5]. It is classified as a BCS Class II drug: its high intestinal permeability is not the limiting factor, but its very low aqueous solubility (approximately 5–7 mg/L) restricts dissolution and, consequently, oral bioavailability [4,6]. This solubility limitation is clinically significant — the 15 mg and 20 mg strengths of rivaroxaban must be administered with food to achieve adequate absorption, a requirement that compromises dosing flexibility and adherence in patients with irregular feeding schedules or swallowing difficulties [7,8].

Lipid-based drug delivery systems, and self-nanoemulsifying drug delivery systems (SNEDDS) in particular, have emerged as a rational formulation

International Journal of Pharmaceutical research and Applications
Volume 11, Issue 5, Sep.-Oct.2026, pp:760-775 www.ijprajournal.com ISSN:2456-4494

strategy for BCS Class II drugs [9,10]. A SNEDDS is an isotropic mixture of drug, oil, surfactant and co-surfactant that spontaneously forms a fine, thermodynamically stable oil-in-water nanoemulsion upon mild agitation in gastrointestinal fluid, presenting the drug in a pre-dissolved, high-surface-area state that favours rapid dissolution and absorption [9–11]. However, conventional liquid SNEDDS (L-SNEDDS) present practical drawbacks — limited stability on storage, capsule-shell compatibility issues, and handling difficulties during large-scale manufacture [12,13]. Converting an optimized liquid SNEDDS into a solid SNEDDS (S-SNEDDS), typically by adsorption onto a porous, high-surface-area solid carrier, retains the self-emulsifying performance of the liquid precursor while conferring the manufacturing, packaging and stability advantages of a conventional solid oral dosage form [12–14].

While liquid SNEDDS approaches to rivaroxaban have been explored in the literature, comparatively little attention has been directed toward converting an optimized rivaroxaban SNEDDS into a solid dosage form using a simple adsorption technique, together with a systematic evaluation of the resulting micromeritic and dissolution behaviour. The present study was therefore undertaken to (i) screen and select a suitable oil, surfactant and co-surfactant for rivaroxaban on the basis of solubility and emulsification efficiency; (ii) construct a pseudo-ternary phase diagram and prepare a series of liquid SNEDDS formulations; (iii) characterize the liquid SNEDDS with respect to thermodynamic stability, dilution robustness, self-emulsification behaviour, viscosity, transmittance, droplet size, polydispersity, zeta potential and drug loading efficiency; (iv) convert the optimized liquid SNEDDS into an S-SNEDDS by adsorption onto Aerosil® 200; and (v) evaluate the micromeritic properties, drug loading efficiency, in vitro release and release kinetics of the optimized S-SNEDDS relative to the pure drug and a marketed tablet.

II. MATERIALS AND METHODS

2.1 Materials and Equipment

Rivaroxaban was obtained ex-gratis from Fourrts India Laboratories Pvt. Ltd. Oleic acid, Tween 80 and polyethylene glycol (PEG) 400 were procured from Loba Chemie Pvt. Ltd. Acetonitrile (HPLC grade) was obtained from Sisco Research Laboratories Pvt. Ltd., and colloidal silicon dioxide (Aerosil® 200) from Yarrow Chem Products Pvt. Ltd. All other chemicals and solvents used were of analytical grade. The materials and principal instruments used in this study are listed in Tables 1 and 2.

Table 1. Materials used in the study

Material	Source
Rivaroxaban	Fourrts India Laboratories Pvt. Ltd.
Oleic acid	Loba Chemie Pvt. Ltd.
Tween 80	Loba Chemie Pvt. Ltd.
Polyethylene glycol 400	Loba Chemie Pvt. Ltd.
Acetonitrile	Sisco Research Laboratories Pvt. Ltd.
Colloidal silicon dioxide (Aerosil® 200)	Yarrow Chem Products Pvt. Ltd.

Table 2. Major equipment used in the study

Equipment	Model / Manufacturer
UV–Visible spectrophotometer	JASCO V-730 / V-750
Magnetic stirrer	REMI 2MLH, Mumbai
Brookfield viscometer	DV-II+ Pro
Analytical balance	MC Dalal, Chennai
pH meter	Eutech Instruments

International Journal of Pharmaceutical research and Applications
Volume 11, Issue 5, Sep.-Oct.2026, pp:760-775 www.ijprajournal.com ISSN:2456-4494

Equipment	Model / Manufacturer
FT-IR spectrophotometer	JASCO FT/IR-4X, Japan
Probe sonicator	Lab India Apparatus, Thane
Dissolution test apparatus	Lab India Apparatus, Thane
Zetasizer	HORIBA SZ-100
Transmission electron microscope	JEM-2100 Plus

2.2 Preformulation Studies

The organoleptic properties (colour, odour, physical form) of rivaroxaban were recorded by direct sensory examination. Melting point was determined in triplicate by the capillary-tube method per USP General Chapter ‹741›, with the temperature ramped at ~1 °C/min near the expected melting range [15]. Aqueous and organic solubility was assessed by the shake-flask method, in which an excess of drug was equilibrated with individual solvents and visually graded for solubility. The wavelength of maximum absorption (λmax) was determined by scanning a 10 µg/mL solution of rivaroxaban in acetonitrile:water (1:1 v/v) between 200 and 400 nm on a JASCO V-730 UV–visible spectrophotometer. A calibration curve was subsequently constructed over 0.5–10 µg/mL in the same solvent system at the selected λmax, and linearity was assessed from the regression coefficient (R^2).

Drug–excipient compatibility was assessed by FT-IR spectroscopy (JASCO FT/IR-4X, 4000–400 cm^{-1}) on KBr discs of the pure drug, 1:1 physical mixtures with each excipient, and the optimized liquid and solid SNEDDS formulations, with the resulting spectra compared for the persistence of characteristic rivaroxaban absorption bands.

2.3 Screening of Oil, Surfactant and Co-Surfactant

The solubility of rivaroxaban in a panel of oils (olive, castor, clove, sesame, peppermint oil and oleic acid), surfactants (Labrasol® ALF, Tween 20, Tween 60, Tween 80, Span 20, Span 80, Cremophor® RH 40) and co-surfactants (PEG 200, PEG 400, PEG 600, polypropylene glycol) was determined by the shake-flask method: an excess of drug was equilibrated with 1 mL of each excipient (40 ± 2 °C, 24 h, followed by 30 ± 2 °C, 72 h), centrifuged (3000 rpm, 20 min), and the supernatant assayed spectrophotometrically at 249 nm after appropriate dilution. The excipient in each category exhibiting maximum drug solubility was carried forward for emulsification-efficiency screening, in which 300 µL of surfactant was mixed with 300 µL of the selected oil, and 200 µL of the resulting mixture was introduced into 100 mL distilled water; the number of gentle flask inversions needed to obtain a homogeneous nanoemulsion and the percentage transmittance at 650 nm (2 h post-dilution) were recorded. An analogous procedure (600 µL oil : 400 µL surfactant : 200 µL co-surfactant) was used to screen co-surfactants against the selected oil–surfactant pair.

2.4 Construction of the Pseudo-Ternary Phase Diagram

Pseudo-ternary phase diagrams were constructed by the aqueous titration method for Smix (Tween 80:PEG 400) weight ratios of 1:1, 1:2 and 2:1. For each Smix ratio, oil and Smix were combined in proportions ranging from 1:9 to 9:1 (w/w) and titrated with water under magnetic stirring; the mixtures were visually classified as transparent/isotropic (nanoemulsion region) or turbid/phase-separated. The diagrams were plotted using Chemix School 11.0 software, and the Smix ratio yielding the largest nanoemulsion region was selected for formulation of the liquid SNEDDS.

2.5 Preparation of Rivaroxaban-Loaded Liquid SNEDDS (F1–F9)

Using the selected Smix ratio, nine liquid SNEDDS formulations (F1–F9) were prepared at oil-to-Smix ratios spanning 1:9 to 9:1 (Table 3), keeping the rivaroxaban dose (10 mg) and final formulation volume (1 mL) constant across all formulations. Rivaroxaban was dispersed in oleic acid under vortex mixing, the pre-mixed Smix (Tween 80 + PEG 400) was added, and the mixture was vortexed (10–15 min), sonicated (10 min) and warmed (40 °C, 30–40 min, intermittent shaking) until a clear, isotropic preconcentrate was obtained. Formulations were stored at room temperature and observed visually for 48 h to exclude turbidity, precipitation or phase separation prior to evaluation.

International Journal of Pharmaceutical research and Applications
Volume 11, Issue 5, Sep.-Oct.2026, pp:760-775 www.ijprajournal.com ISSN:2456-4494

2.6 Characterization of Liquid SNEDDS

The prepared L-SNEDDS formulations were evaluated as follows.

Thermodynamic stability: Formulations were subjected to centrifugation (3500 rpm, 30 min), six heating–cooling cycles (4 and 45 °C, 48 h/cycle) and three freeze–thaw cycles (−20 ± 2 °C and 25 ± 2 °C, 48 h/stage), with visual inspection for phase separation, creaming or cracking after each stress.

Robustness to dilution: 1 mL aliquots of each formulation were diluted 1:10, 1:100 and 1:1000 in distilled water, 0.1 N HCl and phosphate buffer pH 6.8, stirred at 100 rpm (37 °C), and observed after 24 h for phase separation, precipitation or drug crystallization.

Self-emulsification grading and time: Emulsification behaviour was graded (A–E) using the standard USP dissolution-apparatus-II visual grading system [16]. Self-emulsification time was separately recorded as the time required for 1 mL of formulation to form a homogeneous nanoemulsion in 300 mL distilled water (37 ± 0.5 °C, 100 rpm magnetic stirring).

Viscosity and transmittance: Viscosity was measured at 25 ± 0.5 °C using a Brookfield viscometer, both undiluted and after 100-fold aqueous dilution. Percentage transmittance of the 100-fold-diluted formulations was measured spectrophotometrically at 650 nm against a distilled-water blank.

Droplet size, PDI and zeta potential: Mean droplet size and polydispersity index (PDI) were determined by dynamic light scattering (1:1000 dilution, 25 °C, 90° scattering angle), and zeta potential was determined on a 1:1000 aqueous dilution using a Zetasizer (HORIBA SZ-100).

Morphology: The surface morphology and globule shape of the optimized formulation were examined by transmission electron microscopy (1:100 dilution, negative staining with 2% w/v phosphotungstic acid).

Drug loading efficiency: One millilitre of formulation was diluted in acetonitrile:water (1:1 v/v), and the rivaroxaban content was determined spectrophotometrically at 249 nm against the calibration curve; drug loading efficiency (%) was calculated as (actual drug content / theoretical drug content) × 100.

In vitro drug release (dialysis bag method): SNEDDS equivalent to 10 mg rivaroxaban was enclosed in a pre-soaked dialysis membrane and immersed in 900 mL phosphate buffer pH 6.8 (37 ± 0.5 °C, USP Apparatus II, 50 rpm). Samples (5 mL) were withdrawn at fixed intervals up to 60 min, replaced with fresh medium, and analysed spectrophotometrically at 249 nm.

2.7 Conversion to Solid SNEDDS (S-SNEDDS) by Adsorption

The optimized L-SNEDDS (F3) was converted to a free-flowing solid by adsorption onto Aerosil® 200 (colloidal silicon dioxide) in a 1:2 (v/w, SNEDDS:Aerosil® 200) ratio. The liquid preconcentrate was added dropwise to the carrier with continuous trituration in a glass mortar until a uniform powder was obtained, which was dried (40 °C, 2 h) and passed through a #60 mesh sieve.

2.8 Evaluation of S-SNEDDS

Micromeritic properties: Angle of repose (fixed-funnel method), bulk and tapped density, Carr's compressibility index [(TD−BD)/TD × 100] and Hausner's ratio (TD/BD) were determined on the S-SNEDDS powder.

Drug loading efficiency: One gram of S-SNEDDS was extracted with acetonitrile:water (1:1 v/v), and the rivaroxaban content was quantified spectrophotometrically at 249 nm against the calibration curve.

In vitro drug release: Hard gelatin capsules (size '000') containing S-SNEDDS equivalent to 10 mg rivaroxaban were evaluated using USP Apparatus II (900 mL phosphate buffer pH 6.8, 37 ± 0.5 °C, 50 rpm), with capsules anchored using a parafilm-supported spring sinker to prevent floating. Samples (5 mL, replaced with fresh medium) were withdrawn up to 60 min, filtered (0.45 µm), and analysed at 249 nm. Pure rivaroxaban and a marketed rivaroxaban tablet were evaluated under identical conditions for comparison.

Release kinetics: Cumulative release data were fitted to zero-order, first-order, Higuchi and Korsmeyer–Peppas models [17–19], and the model of best fit was identified from the highest regression coefficient (R^2).

2.9 Statistical Treatment

All quantitative measurements were performed in triplicate (n = 3) and are expressed as mean ± standard deviation (SD).

III. RESULTS AND DISCUSSION

3.1 Preformulation Studies

Rivaroxaban was obtained as a white to off-white, odourless crystalline powder, consistent with its reported physical description. The melting point, determined by the capillary-tube method, was found to be 230 °C, in agreement with the reported range for rivaroxaban (228–229 °C). Solubility studies (Table 3) confirmed that rivaroxaban was practically insoluble in distilled water and phosphate buffer pH

International Journal of Pharmaceutical research and Applications
Volume 11, Issue 5, Sep.-Oct.2026, pp:760-775 www.ijprajournal.com ISSN:2456-4494

6.8, very slightly soluble in ethanol, slightly soluble in acetone, and freely soluble in chloroform, DMSO and acetonitrile — a solubility profile consistent with its classification as a BCS Class II compound.

Table 3. Solubility of rivaroxaban in various solvents

Solvent	Solubility
Distilled water	Practically insoluble
Phosphate buffer pH 6.8	Practically insoluble
Ethanol	Very slightly soluble
Acetone	Slightly soluble
Chloroform	Soluble
DMSO	Freely soluble
Acetonitrile	Freely soluble

Scanning of rivaroxaban in acetonitrile:water (1:1 v/v) over 200–400 nm showed maximum absorption at 249 nm, which was adopted as the analytical wavelength for all subsequent spectrophotometric assays. The calibration curve constructed over 0–10 µg/mL (Figure 1) was linear ($y = 0.0331x - 0.0052$, $R^2 = 0.9991$), confirming adherence to the Beer–Lambert law over the working concentration range.

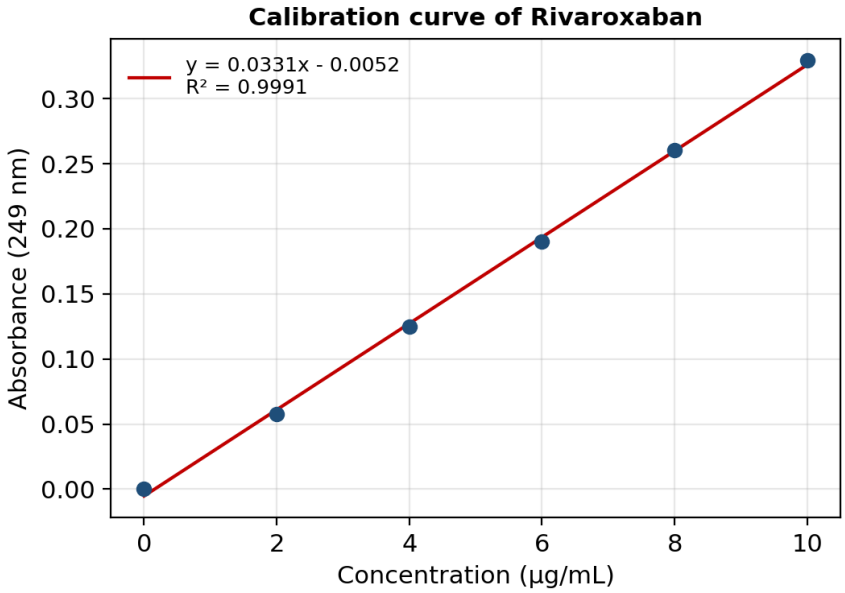

Figure 1. Calibration curve of rivaroxaban in acetonitrile:water (1:1 v/v) at 249 nm.

3.2 Drug–Excipient Compatibility (FT-IR)

FT-IR spectra of pure rivaroxaban, its physical mixtures with oleic acid, Tween 80 and PEG 400, and the optimized L-SNEDDS and S-SNEDDS formulations all retained the characteristic rivaroxaban absorption bands — carbonyl C=O stretching (~1738 cm^{-1}), amide C=O stretching (~1645–1658 cm^{-1}), aromatic C=C stretching (~1548–1550 cm^{-1}), C–N stretching (~1220–1249 cm^{-1}) and C–H bending (~940–997 cm^{-1}). In the optimized S-SNEDDS, the carbonyl band shifted modestly from 1738.5 to 1726.9 cm^{-1}, most likely reflecting non-covalent physical interaction with the surrounding excipients/adsorbent rather than chemical degradation, since no new absorption bands appeared and no characteristic peaks were lost. These findings indicate that rivaroxaban remained

International Journal of Pharmaceutical research and Applications
Volume 11, Issue 5, Sep.-Oct.2026, pp:760-775 www.ijprajournal.com ISSN:2456-4494

chemically compatible with the selected excipients and adsorbent throughout formulation.

3.3 Selection of Oil, Surfactant and Co-Surfactant

Among the oils screened, oleic acid showed the highest rivaroxaban solubility (9.86 mg/mL); among surfactants, Tween 80 showed the highest solubility (12.86 mg/mL); and among co-surfactants, PEG 400 showed the highest solubility (11.83 mg/mL) (Table 4). Oleic acid, Tween 80 and PEG 400 were accordingly selected as the oil, surfactant and co-surfactant, respectively, for SNEDDS development.

Table 4. Solubility of rivaroxaban in screened oils, surfactants and co-surfactants

Category	Excipient	Solubility (mg/mL)
Oil	Olive oil	8.97
Oil	Castor oil	7.62
Oil	Clove oil	5.43
Oil	Sesame oil	3.76
Oil	Peppermint oil	6.75
Oil	Oleic acid ✓ selected	9.86
Surfactant	Labrasol® ALF	6.43
Surfactant	Tween 20	8.94
Surfactant	Tween 60	7.23
Surfactant	Tween 80 ✓ selected	12.86
Surfactant	Span 20	11.09
Surfactant	Span 80	8.64
Surfactant	Cremophor® RH 40	4.76
Co-surfactant	PEG 200	8.51
Co-surfactant	PEG 400 ✓ selected	11.83
Co-surfactant	PEG 600	8.94
Co-surfactant	Polypropylene glycol	10.51

Emulsification-efficiency screening (Table 5) confirmed this selection: Tween 80 produced the clearest nanoemulsion with the fewest inversions (99.87% transmittance, 7 inversions) among surfactants tested, and PEG 400 performed best among co-surfactants (99.66% transmittance, 4 inversions), supporting their selection on the basis of both solubilizing capacity and self-emulsification performance.

Table 5. Emulsification efficiency of screened surfactants and co-surfactants

Excipient	% Transmittance	No. of inversions
Labrasol® ALF	85.62	12
Tween 20	68.37	15
Tween 60	49.28	22
Tween 80 ✓	99.87	7
Span 20	94.36	9

International Journal of Pharmaceutical research and Applications
Volume 11, Issue 5, Sep.-Oct.2026, pp:760-775 www.ijprajournal.com ISSN:2456-4494

Excipient	% Transmittance	No. of inversions
Span 80	82.71	14
Cremophor® RH 40	38.53	10
PEG 200	92.39	9
PEG 400 ✓	99.66	4
PEG 600	91.30	13
Polypropylene glycol	88.93	8

3.4 Pseudo-Ternary Phase Diagram

Phase diagrams constructed for Smix (Tween 80:PEG 400) ratios of 1:1, 1:2 and 2:1 showed that the nanoemulsion (self-emulsifying) region was largest at an Smix ratio of 1:2. At this ratio, the relatively higher proportion of co-surfactant to surfactant is expected to reduce interfacial tension further and increase interfacial fluidity, favouring spontaneous nanoemulsification. An Smix ratio of 1:2 was therefore fixed for preparation of the liquid SNEDDS formulations.

3.5 Composition and Thermodynamic Stability of L-SNEDDS

Nine liquid SNEDDS formulations (F1–F9) were prepared at oil-to-Smix ratios of 1:9 through 9:1 (Table 6), keeping the rivaroxaban dose (10 mg) and total volume (1 mL) constant.

Table 6. Composition of rivaroxaban-loaded liquid SNEDDS formulations (Smix 1:2)

Formula	Oil (µL)	Surfactant (µL)	Co-surfactant (µL)	Oil:Smix ratio
F1	100	300	600	1:9
F2	200	267	533	2:8
F3	300	233	467	3:7
F4	400	200	400	4:6
F5	500	167	333	5:5
F6	600	133	267	6:4
F7	700	100	200	7:3
F8	800	66	134	8:2
F9	900	33	67	9:1

All nine formulations remained physically stable to centrifugation. However, formulations with higher oil content showed progressively poorer tolerance to thermal and freeze–thaw stress: F1–F7 passed all three thermodynamic stability tests, F8 failed the heating–cooling cycle, and F9 failed both the heating–cooling and freeze–thaw cycles (Table 7). Similarly, robustness-to-dilution testing across distilled water, 0.1 N HCl and phosphate buffer pH 6.8 (at 10-, 100- and 1000-fold dilution) showed that F1–F7 remained clear and homogeneous at all dilution levels and media, whereas F8 and F9 showed instability under most dilution conditions. F1–F7 were therefore considered suitable for further evaluation.

Table 7. Thermodynamic stability of rivaroxaban SNEDDS formulae

Formula	Centrifugation	Heating–cooling cycle	Freeze–thaw cycle
F1	Pass	Pass	Pass
F2	Pass	Pass	Pass

International Journal of Pharmaceutical research and Applications
Volume 11, Issue 5, Sep.-Oct.2026, pp:760-775 www.ijprajournal.com ISSN:2456-4494

Formula	Centrifugation	Heating–cooling cycle	Freeze–thaw cycle
F3	Pass	Pass	Pass
F4	Pass	Pass	Pass
F5	Pass	Pass	Pass
F6	Pass	Pass	Pass
F7	Pass	Pass	Pass
F8	Pass	Fail	Pass
F9	Pass	Fail	Fail

3.6 Self-Emulsification, Viscosity and Transmittance

All nine formulations self-emulsified within Grade A or B on visual grading; F1–F5 (lower oil content) formed clear, rapidly dispersing nanoemulsions (Grade A), while F6–F9 (higher oil content) were slightly less clear (Grade B). Self-emulsification time ranged from 22.3 ± 0.75 s (F3) to 84.2 ± 1.88 s (F7), with F3 emulsifying fastest and formulations F6–F9 taking substantially longer, consistent with the higher oil fraction slowing spontaneous dispersion (Table 8).

Table 8. Self-emulsification time of rivaroxaban SNEDDS formulae (mean ± SD, n = 3)

Formula	Self-emulsification time (s)
F1	25.1 ± 0.77
F2	28.6 ± 1.26
F3	22.3 ± 0.75
F4	34.0 ± 0.85
F5	38.7 ± 1.38
F6	65.9 ± 1.13
F7	84.2 ± 1.88
F8	76.5 ± 1.37
F9	80.4 ± 0.92

Undiluted formulation viscosity ranged from 23.35 ± 0.84 to 62.15 ± 1.69 cP, falling to 12.95 ± 1.39–36.72 ± 0.74 cP after 100-fold aqueous dilution — low viscosities consistent with formation of an oil-in-water (o/w) type nanoemulsion favourable to rapid self-emulsification. Percentage transmittance (Table 9) was highest for F3 (99 ± 0.52%), indicating the clearest, most optically isotropic nanoemulsion among the nine formulations, and declined progressively with increasing oil content (F7, 35 ± 0.93%; F9, 25 ± 2.27%).

Table 9. Percentage transmittance of rivaroxaban SNEDDS formulae (650 nm, mean ± SD, n = 3)

Formula	% Transmittance
F1	80 ± 0.47
F2	91 ± 0.38
F3	99 ± 0.52
F4	88 ± 0.71
F5	95 ± 0.63

International Journal of Pharmaceutical research and Applications
Volume 11, Issue 5, Sep.-Oct.2026, pp:760-775 www.ijprajournal.com ISSN:2456-4494

Formula	% Transmittance
F6	70 ± 1.04
F7	35 ± 0.93
F8	60 ± 0.18
F9	25 ± 2.27

3.7 Droplet Size, Polydispersity Index and Zeta Potential

All nine formulations produced droplets under 200 nm, confirming their suitability as SNEDDS. Mean droplet size ranged from 95.3 nm (F3) to 171.8 nm (F9), and PDI ranged from 0.257 (F3) to 0.521 (F9) (Table 10, Figure 2) — both parameters increasing monotonically with oil content, indicating progressively less uniform droplet populations as the proportion of oil in the formulation rose. Zeta potential ranged from −20.8 mV (F9) to −41.4 mV (F3) (Table 10, Figure 3); F3 showed the highest magnitude negative charge, suggesting comparatively stronger electrostatic repulsion between droplets and, correspondingly, better colloidal stability. Transmission electron microscopy of the optimized F3 formulation (after aqueous dilution) showed predominantly spherical, well-dispersed globules without significant aggregation, corroborating the droplet-size and PDI results.

Table 10. Droplet size, PDI and zeta potential of rivaroxaban SNEDDS formulae

Formula	Droplet size (nm)	PDI	Zeta potential (mV)
F1	118.6	0.346	−31.8
F2	106.9	0.294	−36.5
F3	95.3	0.257	−41.4
F4	101.5	0.278	−38.2
F5	112.8	0.322	−34.6
F6	128.4	0.389	−29.7
F7	142.7	0.432	−26.4
F8	156.3	0.476	−22.9
F9	171.8	0.521	−20.8

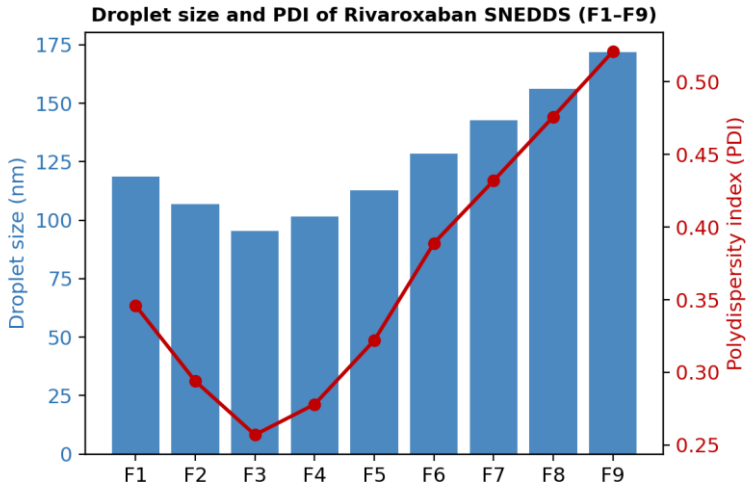

International Journal of Pharmaceutical research and Applications
Volume 11, Issue 5, Sep.-Oct.2026, pp:760-775 www.ijprajournal.com ISSN:2456-4494

Figure 2. Droplet size and PDI of rivaroxaban SNEDDS formulations (F1–F9).

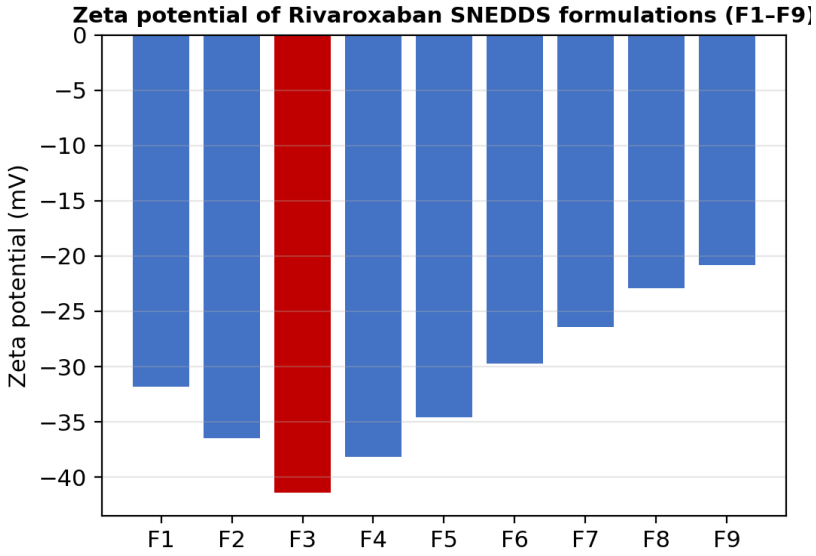

Figure 3. Zeta potential of rivaroxaban SNEDDS formulations (F1–F9).

3.8 Drug Loading Efficiency and In Vitro Release of L-SNEDDS

Drug loading efficiency of the nine formulations ranged from 71.68 ± 0.56% (F9) to 98.43 ± 0.02% (F3) (Table 11), the highest value coinciding with the Smix concentration and droplet characteristics of F3, consistent with its superior solubilizing environment for rivaroxaban.

Table 11. Drug loading efficiency of rivaroxaban L-SNEDDS formulae (mean ± SD, n = 3)

Formula	Drug loading efficiency (%)
F1	90.84 ± 0.43
F2	85.62 ± 0.28
F3	98.43 ± 0.02
F4	92.71 ± 0.24
F5	83.56 ± 0.37
F6	75.97 ± 0.51
F7	82.73 ± 0.62
F8	78.95 ± 0.48
F9	71.68 ± 0.56

In vitro release from the dialysis-bag method (Table 12, Figure 4) showed F3 releasing 97.8% of rivaroxaban at 60 min — the highest among all nine formulations — with the fastest onset (31.8% at 5 min versus 13.8–21.0% for the other formulations). This is consistent with F3's smallest droplet size and highest transmittance, both of which increase the interfacial surface area available for drug release. On the basis of its self-emulsification time, transmittance, droplet size, PDI, zeta potential, drug loading efficiency and release performance considered together, F3 (oil:Smix, 3:7) was selected as the optimized liquid SNEDDS formulation for conversion into S-SNEDDS.

International Journal of Pharmaceutical research and Applications
Volume 11, Issue 5, Sep.-Oct.2026, pp:760-775 www.ijprajournal.com ISSN:2456-4494

Table 12. In vitro cumulative drug release (%) of rivaroxaban L-SNEDDS formulae (mean ± SD, n = 3)

Time (min)	F1	F2	F3	F4	F5	F6	F7	F8	F9
0	0	0	0	0	0	0	0	0	0
5	16.8	20.1	31.8	18.4	21.0	17.6	18.9	14.7	13.8
10	28.4	31.6	49.7	30.2	33.1	29.0	30.6	23.8	22.4
15	40.2	43.8	66.5	41.1	45.0	39.5	41.7	32.6	31.0
20	49.8	55.0	78.2	52.4	57.1	50.6	49.9	41.8	39.7
30	61.5	67.8	89.0	64.0	69.2	62.1	53.4	52.4	49.8
45	78.4	70.2	95.1	79.6	80.8	70.6	57.8	74.2	61.5
60	90.0	76.0	97.8	92.0	87.0	74.0	62.0	84.0	71.0

Values are mean cumulative percentage drug release (n = 3); SD omitted from the table for compactness (range 0.36–1.45 percentage points across formulations and time points) but retained in the primary laboratory records.

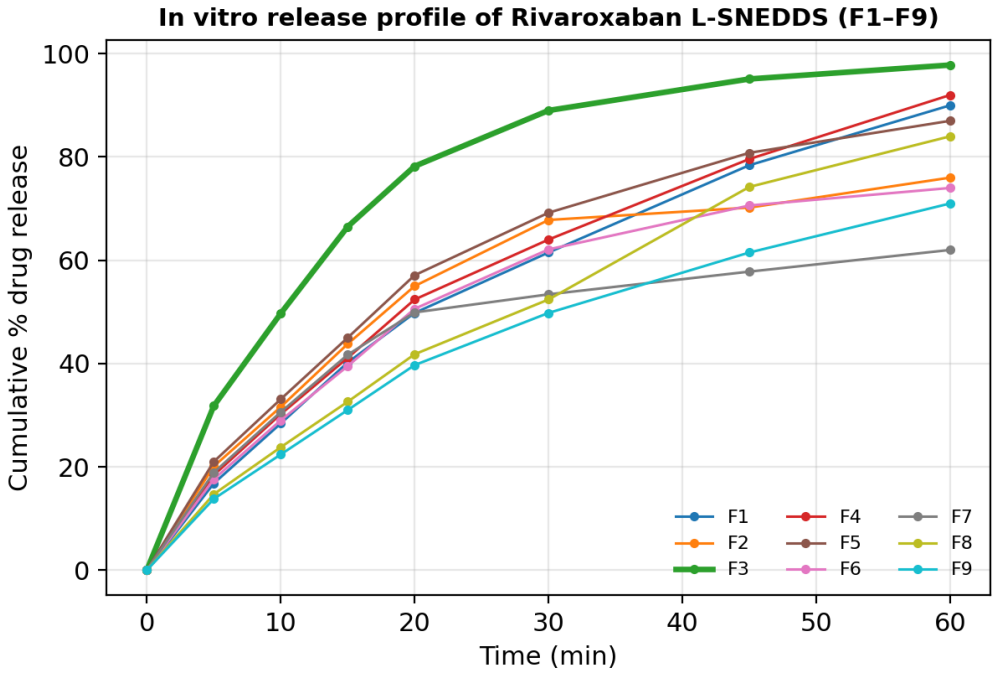

Figure 4. In vitro release profile of rivaroxaban L-SNEDDS (F1–F9), dialysis bag method, phosphate buffer pH 6.8.

3.9 Conversion to S-SNEDDS and Micromeritic Evaluation

The optimized L-SNEDDS (F3) was converted into a free-flowing S-SNEDDS by adsorption onto Aerosil® 200 (1:2, v/w). The resulting powder showed an angle of repose of 26.59°, bulk density of 0.48 g/mL, tapped density of 0.58 g/mL, Carr's index of 17.2% and Hausner's ratio of 1.20 (Table 13) — values consistent with good powder flowability, likely reflecting the relatively spherical particle morphology imparted by the adsorption process.

International Journal of Pharmaceutical research and Applications
Volume 11, Issue 5, Sep.-Oct.2026, pp:760-775 www.ijprajournal.com ISSN:2456-4494

Table 13. Micromeritic properties of the optimized rivaroxaban S-SNEDDS (F3)

Parameter	Value
Angle of repose	26.59°
Bulk density	0.48 g/mL
Tapped density	0.58 g/mL
Carr's index	17.2%
Hausner's ratio	1.20
Drug loading efficiency	95.43 ± 0.02%

The drug loading efficiency of the S-SNEDDS (95.43 ± 0.02%) was comparable to that of the parent L-SNEDDS (98.43 ± 0.02%), indicating that adsorption onto Aerosil® 200 did not result in appreciable loss of rivaroxaban during solidification.

3.10 Comparative In Vitro Drug Release

The optimized S-SNEDDS showed markedly higher in vitro release than both pure rivaroxaban and a marketed rivaroxaban tablet under identical dissolution conditions (Table 14, Figure 5). At 60 min, the S-SNEDDS released 97.24 ± 0.74% of the labelled dose, compared with 75.0 ± 2.7% for the marketed tablet and only 50.0 ± 2.5% for pure drug. The S-SNEDDS also showed markedly faster onset (28.42 ± 0.32% released at 5 min, versus 17.9 ± 1.8% for the marketed tablet and 8.2 ± 1.2% for pure drug), consistent with rapid in situ nanoemulsification of the adsorbed formulation on contact with the dissolution medium, presenting rivaroxaban in a pre-solubilized, high-surface-area state.

Table 14. Comparative in vitro cumulative drug release (%): pure rivaroxaban, marketed tablet and optimized S-SNEDDS (mean ± SD, n = 3)

Time (min)	Pure drug	Marketed tablet	S-SNEDDS
0	0	0	0
5	8.2 ± 1.2	17.9 ± 1.8	28.42 ± 0.32
10	16.9 ± 1.5	33.8 ± 2.0	46.84 ± 0.41
15	24.6 ± 1.8	47.9 ± 2.2	63.25 ± 0.48
20	31.8 ± 1.9	58.0 ± 2.4	75.62 ± 0.55
30	40.2 ± 2.1	66.1 ± 2.5	88.34 ± 0.61
45	46.0 ± 2.3	72.3 ± 2.6	94.18 ± 0.68
60	50.0 ± 2.5	75.0 ± 2.7	97.24 ± 0.74

International Journal of Pharmaceutical research and Applications
Volume 11, Issue 5, Sep.-Oct.2026, pp:760-775 www.ijprajournal.com ISSN:2456-4494

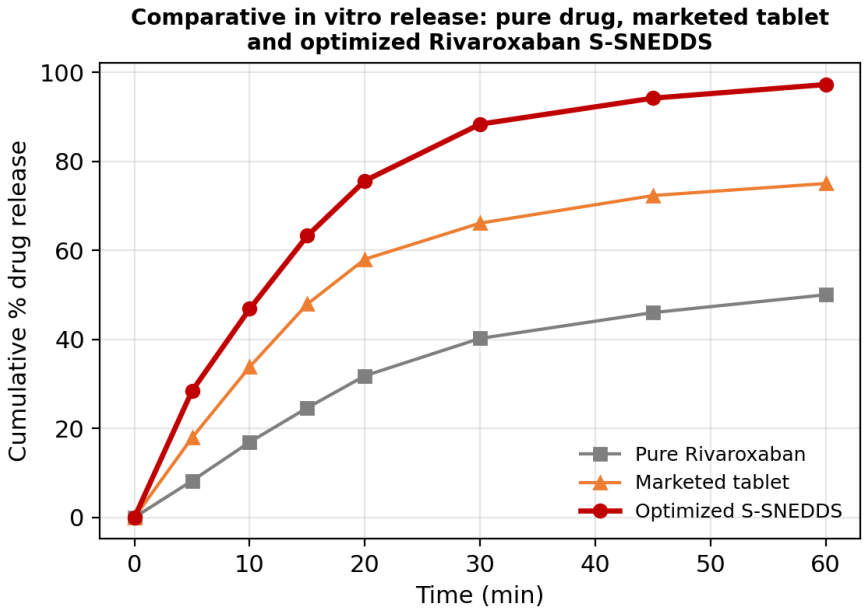

Figure 5. Comparative in vitro release of pure rivaroxaban, marketed tablet and optimized S-SNEDDS.

3.11 Release Kinetics

Release data from the optimized S-SNEDDS were fitted to zero-order, first-order, Higuchi and Korsmeyer–Peppas models (Table 15). The first-order model gave the best fit ($R^2 = 0.9676$), indicating that drug release from the S-SNEDDS was predominantly concentration-dependent, consistent with rapid, near-complete nanoemulsification and dissolution of the adsorbed drug within the early sampling intervals. The zero-order and Higuchi fits ($R^2 = 0.9358$ each) were markedly lower than the first-order fit; the Korsmeyer–Peppas model gave the poorest fit ($R^2 = 0.8663$), with a release exponent ($n = 1.3925$) outside the range normally used to assign a discrete diffusional mechanism, and is accordingly interpreted with caution.

Table 15. Release-kinetic model parameters for the optimized rivaroxaban S-SNEDDS

Model	R^2	Slope	k
Zero-order	0.9358	13.647	0.3246
First-order	0.9676	−0.2218	2.3468
Higuchi	0.9358	13.647	0.3246
Korsmeyer–Peppas	0.8663	0.0846	1.3925

Note: the Higuchi and zero-order rows carry identical slope and R^2 values in the underlying laboratory data sheet. As the Higuchi model (cumulative % release vs. √time) and the zero-order model (cumulative % release vs. time) use different abscissae, an exact numerical match is not expected on independent regression, and this coincidence is flagged here as an unresolved data-entry artefact in the original dataset rather than silently corrected or re-derived.

International Journal of Pharmaceutical research and Applications
Volume 11, Issue 5, Sep.-Oct.2026, pp:760-775 www.ijprajournal.com ISSN:2456-4494

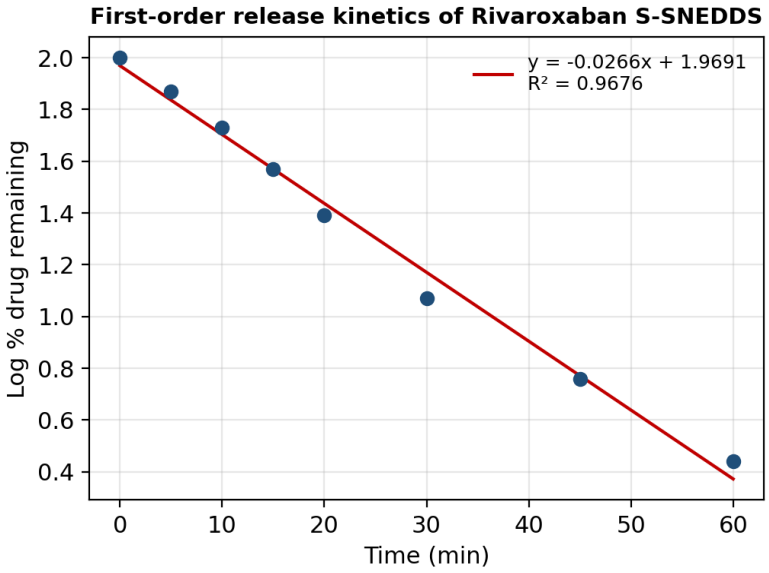

Figure 6. First-order release-kinetic plot for the optimized rivaroxaban S-SNEDDS.

3.12 Comparison with Recent Literature

The performance of the present rivaroxaban S-SNEDDS is broadly consistent with recent (2024–2025) reports on solid SNEDDS of other poorly water-soluble drugs. Jang et al. reported a carvedilol S-SNEDDS solidified using mesoporous silica nanoparticles that achieved roughly 5.7-fold higher dissolution than carvedilol alone, alongside substantial pharmacokinetic gains [20]. Kumar et al. converted nimodipine liquid SNEDDS into solid formulations using chitosan–EDTA microparticle adsorbents, obtaining satisfactory flow properties and markedly improved dissolution relative to pure drug [21], while a related study by the same group applied an analogous adsorption strategy to cyclosporine [22]. More et al. optimized a rhein S-SNEDDS (eucalyptus oil, Tween 80, PEG 400) by factorial design, reporting a droplet size of 129.3 ± 1.57 nm and zeta potential of −24.6 ± 0.34 mV [23], values in the same general range as, though somewhat larger and less electronegative than, the optimized F3 formulation in the present study. Shahba et al. demonstrated that a multi-layer self-nanoemulsifying pellet strategy could achieve over 86% drug release within 60 min for ramipril and thymoquinone while improving handling and stability [24], and Merchant et al. showed that functionalized calcium carbonate could similarly solidify supersaturated SNEDDS while preserving self-nanoemulsifying character [25]. Collectively, these precedents support adsorption-based solidification, as used here with Aerosil® 200, as a generalizable and reproducible strategy for translating a well-optimized liquid SNEDDS into a solid dosage form without material loss of dissolution advantage — consistent with the 97.24 ± 0.74% release at 60 min and comparable drug loading efficiency (95.43 ± 0.02% vs. 98.43 ± 0.02% in the liquid precursor) observed for the rivaroxaban S-SNEDDS developed in this work.

IV. CONCLUSION

A rivaroxaban-loaded solid self-nanoemulsifying drug delivery system was successfully developed to address the dissolution limitation associated with this BCS Class II anticoagulant. Systematic screening identified oleic acid, Tween 80 and PEG 400 as a suitable oil, surfactant and co-surfactant, and a liquid SNEDDS prepared at an oil:Smix ratio of 3:7 (F3) showed the smallest droplet size (95.3 nm), lowest PDI (0.257), highest negative zeta potential (−41.4 mV) and highest drug loading efficiency (98.43 ± 0.02%) among nine formulations evaluated. Conversion of F3 into a solid SNEDDS by adsorption onto Aerosil® 200 yielded a free-flowing powder with satisfactory micromeritic properties and comparable drug loading efficiency (95.43 ± 0.02%), and the resulting S-SNEDDS achieved 97.24 ± 0.74% in vitro drug release at 60 min — substantially higher than pure rivaroxaban (50.0 ± 2.5%) and a marketed tablet (75.0 ± 2.7%) — with release best described by first-order kinetics. These in vitro findings indicate that adsorption-based S-SNEDDS is a practical and reproducible formulation approach for enhancing the

dissolution of rivaroxaban, and provide a rational basis for further preclinical pharmacokinetic, stability and bioavailability evaluation of the developed system.

V. DECLARATIONS

Conflict of Interest: The authors declare no conflict of interest.

Funding: This research did not receive any specific grant from funding agencies in the public, commercial, or not-for-profit sectors.

Ethical Approval: Not applicable — this study involved only in vitro formulation and evaluation work and did not involve human participants or animals.

Acknowledgements: The authors thank the Department of Pharmaceutics, Sri Ramakrishna Institute of Paramedical Sciences, College of Pharmacy, Coimbatore, for providing the facilities used in this work, and Fourrts India Laboratories Pvt. Ltd. for the gift sample of rivaroxaban.

REFERENCES

[1]. Kalepu S, Nekkanti V. Insoluble drug delivery strategies: review of recent advances and business prospects. Acta Pharm Sin B. 2015;5(5):442–53.

[2]. Savjani KT, Gajjar AK, Savjani JK. Drug solubility: importance and enhancement techniques. ISRN Pharm. 2012;2012:195727.

[3]. Dokoumetzidis A, Macheras P. A century of dissolution research: from Noyes and Whitney to the Biopharmaceutics Classification System. Int J Pharm. 2006;321(1–2):1–11.

[4]. Perzborn E, Roehrig S, Straub A, Kubitza D, Misselwitz F. The discovery and development of rivaroxaban, an oral, direct factor Xa inhibitor. Nat Rev Drug Discov. 2011;10(1):61–75.

[5]. Bauersachs R, Berkowitz SD, Brenner B, Buller HR, Decousus H, Gallus AS, et al. Oral rivaroxaban for symptomatic venous thromboembolism. N Engl J Med. 2010;363(26):2499–510.

[6]. Kubitza D, Becka M, Wensing G, Voith B, Zuehlsdorf M. Safety, pharmacodynamics, and pharmacokinetics of BAY 59-7939 — an oral, direct Factor Xa inhibitor — after multiple dosing in healthy male subjects. Eur J Clin Pharmacol. 2005;61(12):873–80.

[7]. Stampfuss J, Kubitza D, Becka M, Mueck W. The effect of food on the absorption and pharmacokinetics of rivaroxaban. Int J Clin Pharmacol Ther. 2013;51(7):549–61.

[8]. Mueck W, Stampfuss J, Kubitza D, Becka M. Clinical pharmacokinetic and pharmacodynamic profile of rivaroxaban. Clin Pharmacokinet. 2014;53(1):1–16.

[9]. Pouton CW. Formulation of poorly water-soluble drugs for oral administration: physicochemical and physiological issues and the lipid formulation classification system. Eur J Pharm Sci. 2006;29(3–4):278–87.

[10]. Porter CJH, Trevaskis NL, Charman WN. Lipids and lipid-based formulations: optimizing the oral delivery of lipophilic drugs. Nat Rev Drug Discov. 2007;6(3):231–48.

[11]. Gursoy RN, Benita S. Self-emulsifying drug delivery systems (SEDDS) for improved oral delivery of lipophilic drugs. Biomed Pharmacother. 2004;58(3):173–82.

[12]. Jannin V, Musakhanian J, Marchaud D. Approaches for the development of solid and semi-solid lipid-based formulations. Adv Drug Deliv Rev. 2008;60(6):734–46.

[13]. Tang B, Cheng G, Gu JC, Xu CH. Development of solid self-emulsifying drug delivery systems: preparation techniques and dosage forms. Drug Discov Today. 2008;13(13–14):606–12.

[14]. Bansal T, Mustafa G, Khan ZI, Ahmad FJ, Khar RK, Talegaonkar S. Solid self-nanoemulsifying delivery systems as a platform technology for formulation of poorly soluble drugs. Crit Rev Ther Drug Carrier Syst. 2008;25(1):63–116.

[15]. United States Pharmacopeia. General Chapter ‹741›: Melting Range or Temperature. USP–NF. Rockville (MD): United States Pharmacopeia; 2026.

[16]. Rehman FU, Shah KU, Shah SU, Khan IU, Khan GM, Khan A. From nanoemulsions to self-nanoemulsions, with recent advances in self-nanoemulsifying drug delivery systems (SNEDDS). Expert Opin Drug Deliv. 2017;14(11):1325–40.

[17]. Dash S, Murthy PN, Nath L, Chowdhury P. Kinetic modeling on drug release from controlled drug delivery systems. Acta Pol Pharm. 2010;67(3):217–23.

[18]. Higuchi T. Mechanism of sustained-action medication. Theoretical analysis of rate of release of solid drugs dispersed in solid matrices. J Pharm Sci. 1963;52(12):1145–9.

[19]. Korsmeyer RW, Gurny R, Doelker E, Buri P, Peppas NA. Mechanisms of solute release

from porous hydrophilic polymers. Int J Pharm. 1983;15(1):25–35.

[20]. Jang H, Kim N, Jin SG. Development of a carvedilol-loaded solid self-nanoemulsifying system with increased solubility and bioavailability using mesoporous silica nanoparticles. Int J Mol Sci. 2025;26(4):1592.

[21]. Kumar M, Chawla PA, Faruk A, Chawla V. Solid self-nanoemulsifying drug delivery systems of nimodipine: development and evaluation. Future J Pharm Sci. 2024;10:87.

[22]. Kumar M, Chawla PA, Faruk A, Chawla V. Design and evaluation of solid self-nanoemulsifying drug delivery systems of cyclosporine developed with a superior adsorbent base. RSC Pharm. 2025;2:318.

[23]. More SM, Rashid MA, Kharwade RS, Taha M, Alhamhoom Y, Elhassan GO, et al. Development of solid self-nanoemulsifying drug delivery system of rhein to improve biopharmaceutical performance: physiochemical characterization, and pharmacokinetic evaluation. Int J Nanomedicine. 2025;20:267–91.

[24]. Shahba AA-W, Sherif AY, Elzayat EM, Ali S, Kazi M. Physical isolation strategy in multi-layer self-nanoemulsifying pellets: improving dissolution and drug loading efficiency of ramipril. J Pharm Sci. 2025;114(2):1326–41.

[25]. Merchant J, Müllertz A, Rades T, Bannow J. Functionalized calcium carbonate (FCC) as a novel carrier to solidify supersaturated self-nanoemulsifying drug delivery systems (super-SNEDDS). Eur J Pharm Biopharm. 2023;193:198–207.